Dielectric characterization of the phase transitions in Pb1-y/2(Zr1-xTix)1-yNbyO3(0.03≤x≤0.04, 0.02≤y≤0.05)

Duan, Ning; Cereceda, Noé; Noheda, Beatriz; Gonzalo, Julio A.

Published in:
Journal of Applied Physics

DOI:
10.1063/1.365772

Publication date:
1997

Dielectric characterization of the phase transitions in $Pb_{1-y/2}(Zr_{1-x}Ti_x)_{1-y}Nb_yO_3(0.03 \leqslant x \leqslant 0.04,\ 0.02 \leqslant y \leqslant 0.05)$

Ning Duan,[a] Noé Cereceda, Beatriz Noheda, and Julio A. Gonzalo[b]
Departamento de Fisica de Materiales, C -IV, Universidad Autónoma de Madrid, 28049 Madrid, Spain

(Received 26 November 1996; accepted for publication 15 April 1997)

The Curie temperature and the ideal thermal hysteresis of $Pb_{1-y/2}(Zr_{1-x}Ti_x)_{1-y}Nb_yO_3$ ($0.03 \leqslant x \leqslant 0.04$, $0.02 \leqslant y \leqslant 0.05$) ferroelectric ceramics have been investigated as a function of composition at the $F_{RH}-P_C$ phase transition. Experimental results are analyzed using the generalized effective field approach and taking into account the composition dependence of the dimensionless parameters g and h corresponding to the second and third terms in the generalized effective field expansion. With this approach we can describe reasonably well the composition dependence of $T_C(x,y)$ at the $F_{RH}-P_C$ transition and thermal hysteresis $\Delta T(x,y)$ in the narrow range of compositions investigated. The effects of the oxygen octahedra tilt in the dielectric constant at the $F_{RL}-F_{RH}$ transition have also been investigated as a function of composition. © *1997 American Institute of Physics.* [S0021-8979(97)03614-1]

I. INTRODUCTION

Solid solutions of lead zirconate titanate $Pb(Zr_{1-x}Ti_x)O_3$ (denoted PZT) are ferroelectric ceramic materials with perovskite structure which have important practical applications in high ϵ capacitors, infrared pyroelectric detectors, piezoelectric devices, and ferroelectric memories, using their outstanding ferroelectric, piezoelectric, and pyroelectric properties.

Early studies were focused on the morphotropic phase boundary (MPB), where the piezoelectric electromechanical coupling factor is very high and shows anomalous behavior. In recent years, efforts have been devoted to the Zr-rich PZT range of compositions, due to the abundant phase boundaries between phases, including orthorhombic antiferroelectric (A_O), high temperature rhombohedral ferroelectric (F_{RH}), low-temperature rhombohedral ferroelectric (F_{RI}), and paraelectric (P_C) phases.[1–4] In particular, the rhombohedral ferroelectric region has attracted considerable interest. The $F_{RL}-F_{RH}$ phase transition was first discovered by Barnett in 1962.[5] The structures of the F_{RH} and F_{RL} phases were later reported by Glazer and Mabud.[6] In these phases one finds rotations and distortions of the oxygen octahedron (F_{RL} phase) and only distortions (F_{RH} phase), respectively, in addition to the cation shifts. Later, several studies in the F_{RL} and the F_{RH} structures were performed.[7–9] These results indicated that the increase of the spontaneous polarization near the $F_{RL}-F_{RH}$ phase transition is related to the O_3 tilt coupling to cation shifts along $\langle 111 \rangle$ axis, and depends on the composition (Ti content) and the dopant content. Along with the structural research, other physical properties at the $F_{RL}-F_{RH}$ phase transition have also been investigated.[10] It was found that the $F_{RL}-F_{RH}$ transition has the following features: (a) the transition temperature is close to room temperature; (b) there are small variations in dielectric constant through the transformation; (c) there is a considerable pyroelectric effect during the transition ($\Delta P \approx 2\ \mu C/cm^2$, being the pyroelectric coefficient $\sim 10^{-7}\ \mu C/cm^2\ ^\circ C$, higher than the usual value, which is around $10^{-8}\ \mu C/cm^2\ ^\circ C$). Applications based on the above outstanding properties of the $F_{RL}-F_{RH}$ phase transition are, for example, direct energy conversion from heat to electricity through the $F_{RL}-F_{RH}$ phase transition[11,12] and its use in infrared detectors. Recently, Zr-rich PZT thin films with $F_{RL}-F_{RH}$ phase transitions have been reported to possess prospective potentialities in the fields of IR detectors, energy converters, and uncooled imaging systems.[13]

On the other hand, the use of different dopants allows the enhancement of specific properties and therefore results in wider applications. In the case of Nb doping, for instance, substitution of a small amount of Nb^{5+} for Zr^{4+} (or Ti^{4+}) increases the bulk resistivity and reduces aging effects, because of the difference in chemical valence between Nb^{5+} and Zr^{4+}, which creates a considerable amount of lead vacancies.[14–17] The phase diagram of Nb-doped Zr-rich PZT has been precisely measured.[18–20] The results show that small amounts of Nb dopant shift the ferro-para phase boundary down, and displace the $F_{RL}-F_{RH}$ phase boundary to the left.

In this investigation, the composition dependence of the $F_{RL}-P_C$ and $F_{RL}-F_{RH}$ transition temperatures and the thermal hysteresis which accompanies the transitions have been investigated o a set of compositions with x in the range of (0.03, 0.04) and y in the range of (0.02, 0.05). The results have been analyzed in terms of the generalized effective theory used previously to study the composition dependence of $T(x)$ for samples with a fixed small amount of Nb ($y=0.026$). It may be noted that an important motivation for this work was to investigate the changes in the transition temperature of Zr-rich PZT with varying content of Ti and Nb, since the latter substantially enhances the resistivity of the material, which has important consequences in connection with its use as an energy converter of thermal into electrical energy. A larger internal resistance results in larger power output being obtainable. The range of Nb content has

[a]On leave from Shanghai Institute of Ceramics, CAS.
[b]Electronic mail: julio.gonzalo@uam.es

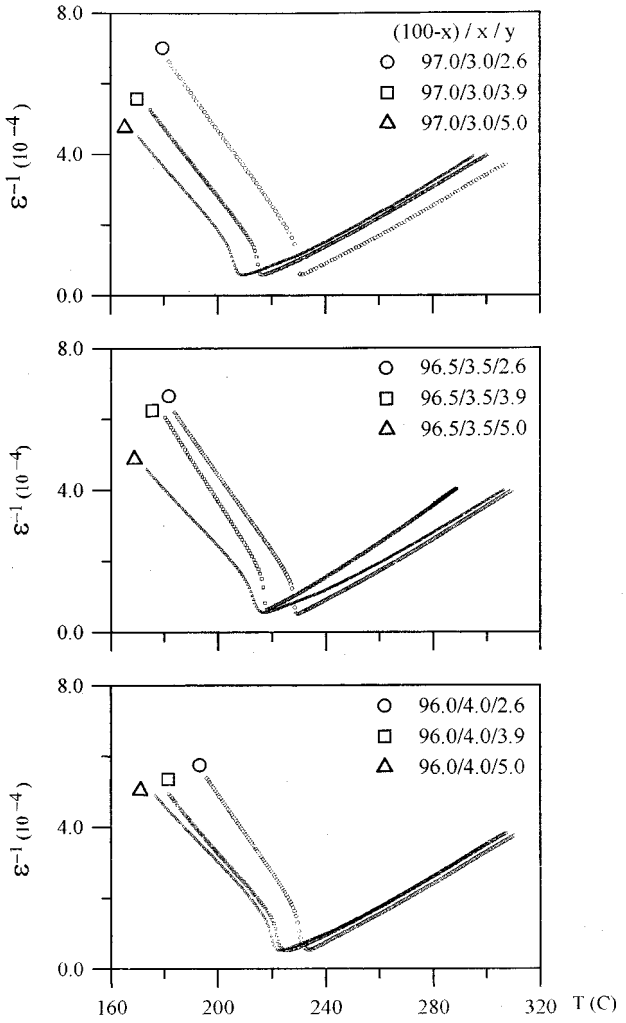

FIG. 1. Dielectric behavior vs temperature for various $Pb_{1-y/2}(Zr_{1-x}Ti_x)_{1-y}Nb_yO_3$ compositions with $0.03 \leqslant x \leqslant 0.04$ and $0.02 \leqslant y \leqslant 0.05$ for the $F_{RH}-P_C$ phase transition.

been chosen to get $F_{RL}-F_{RH}$ transitions in a narrow range not much higher than room temperature.

II. EXPERIMENT

The samples were prepared by the conventional ceramic process in Shanghai Institute of Ceramics, China. They were calcined at 850 °C for 2 h and sintered at 1340 °C for 2 h, then polished into thin disks (thickness of 1 mm, diameter of 1.49 cm) for latter use. Dielectric constant data, capacitance, and dissipation factor, were measured at regular temperature intervals separated by about 0.1 °C, being the temperature controlled by an Eurotherm Temperature Controller/Programmer with a high resolution ramp (Model 903P/IS/HDV) by means of an automatic Hewlett–Packard Precision LCR Meter (Model 4248A) with an accuracy of better than one part in 10^4 at a frequency of 1 kHz. The field amplitude was 8.0 V/cm. The heating and cooling rates were of the order of 20 °C/h, between room temperature and 300 °C.

III. RESULTS AND DISCUSSION

Figure 1 shows the behavior of the inverse dielectric constant with temperature for different compositions around the $F_{RL}-P_C$ transition. From these data the ferro–paraelectric phase transition temperature, T^*, and the Curie temperature, T_C, can be obtained directly. The temperature at which ϵ^{-1} begins to decrease nonlinearly upon heating is defined as T^*. The slope of ϵ^{-1} vs T above T^* was fitted in a narrow temperature range near T^*. The Curie temperature, T_C, is subsequently obtained extrapolating linearly $\epsilon^{-1}(T) \rightarrow 0$. It can be seen that T_C and T^* decrease with the increase of Nb content, y. The experimental results for T^*, T_C, and $\Delta T = T^* - T_C$, corresponding to different niobium contents, are presented in Table I along with the dependence on Ti content. This notation for the extrapolated Curie–Weiss temperature (T_C) and the transition temperature ($T^* \geqslant T_C$) is the same as that used in our previously published work[21] but differs from that used by other authors, which is T_0 and T_C, respectively, for the Curie temperature and the transition temperature.

We may note that there is some diffuse character in the transition peaks, increasing with the Nb content, which may be attributable to small inhomogeneities in composition.[22–24] However, measurements at different frequencies below 1 MHz show that the peak temperature is not seriously affected by the change in frequency, which may be taken as an indication that the diffuse character is not very pronounced in our samples. It allows us to determine the transition and Curie temperatures within a moderate error range. Estimated asymmetric error bars, which vary from composition to composition and are larger when the Nb content is large, are given in the figures.

Figure 2 shows the dielectric constant and losses factor for the $F_{RL}-F_{RH}$ transition. The temperature corresponding to the dielectric constant and the losses factor peak value *is* well defined as the low–high transition temperature, T_{LH}, but the corresponding $F_{RL}-F_{RH}$ ''Curie temperature'', T_{CT}, associated with a hypothetic Curie–Weiss behavior at $T > T_{LH}$, cannot be obtained directly from our data. Taking into account that T_{LH} increases with the increase of Nb and Ti content, T_{CT} could be expected to increase with increasing Nb and Ti content, but this point needs further study.

TABLE I. Experimental data for T^*, T_C, ΔT (all in K) for different $Pb_{1-y/2}(Zr_{1-x}Ti_x)_{1-y}Nb_yO_3$ $(0.03 \leqslant x \leqslant 0.04,\ 0.026 \leqslant y \leqslant 0.05)$ compositions.

y (mol %)→	2.6			3.9			5.0		
$(100-x)/x\downarrow$	T^*	T_C	ΔT	T^*	T_C	ΔT	T^*	T_C	ΔT
97/3	503.5	489.9	13.6	487.8	473.3	14.5	478.1	458.7	19.4
96.5/3.5	501.7	491.2	10.5	489.3	475.1	14.2	484.8	470.1	14.7
96/4	502.8	493.9	8.9	494.5	478.4	16.1	492.5	479.7	12.8

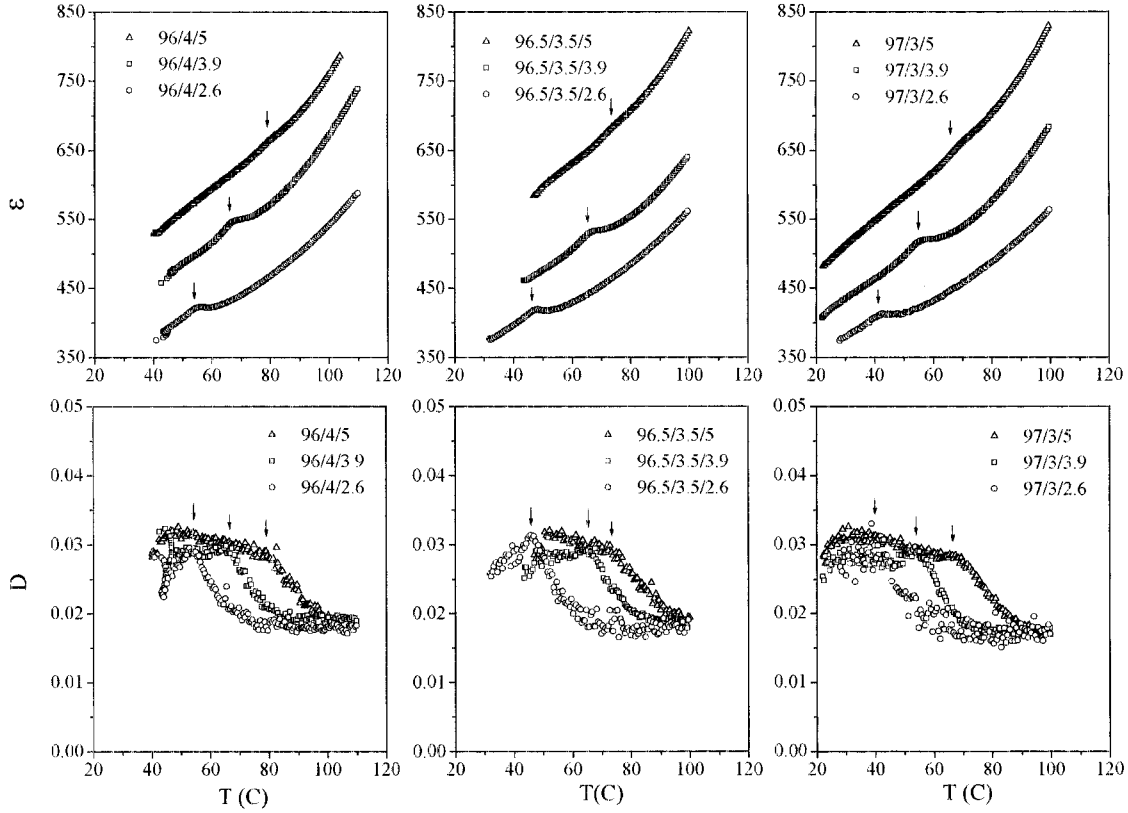

FIG. 2. Dielectric behavior and losses factor vs temperature for the same composition as in Fig. 1 at the $F_{RL}-F_{RH}$ phase transition.

The behaviors described in Fig. 1 and Table I can be analyzed in the framework of the generalized effective field theory,[25] using an effective field

$$E_{\text{eff}}=E+\beta P+\gamma P^3+\delta P^5+\cdots, \tag{1}$$

where E is the external field, P the polarization, and β, γ, δ are constants, i.e., temperature-independent coefficients.

With the substitution of the dimensionless variables $e \equiv E/\beta N\mu$, normalized field; $p\equiv P/N\mu$, normalized polarization; $T_C\equiv\beta N\mu^2/k_B$; $g\equiv(\gamma/\beta)N^2\mu^2$; and $h \equiv(\delta/\beta)N^4\mu^4$, where N is the dipoles number per unit volume, μ the dipole moment per unit cell, and k_B the Boltzmann constant, we get the following equation of state for a pure system:

$$e=\frac{T}{T_C}\tanh^{-1}\, p-p(1+gp^2+hp^4+\cdots). \tag{2}$$

For $e=0$, $p=p_s$ (spontaneous polarization), the above equation is rewritten as

$$\frac{T}{T_C}=\frac{1+gp_s^2+hp_s^4}{\tanh^{-1}\, p_s/p_s}. \tag{3}$$

If we consider a mixed system, like Nb-doped PZT, g and h become composition dependent, as we will discuss below. Thus Eq. (3) can be used to describe the composition dependence of the $F_{RH}-P_C$ phase transition temperature.

A. Composition dependence of the $F_{RH}-P_C$ phase transition

We have pointed out, just before Eq. (2), that T_C for a ferroelectric compound has a linear dependence on the number of dipoles per unit volume, N. So, for a mixed system, a linear dependence of T_C on the molar content, x or y, of the components can be supposed, if we consider the parameters involved, $\{\beta_i\}$ and $\{\mu_i\}$, to be approximately constant in relatively narrow ranges of x and y. The compositions that we have investigated in this work are so close to each other that this constancy can be reasonably assumed. T_C is, then, expressed by means of linear relationships in x and y. As a first approximation,[21]

$$T_C(x,\tilde{y})=T_C(0,\tilde{y})[(1-x)+A_x x] \quad \tilde{y}=\text{constant}, \tag{4}$$

$$T_C(\tilde{x},y)=T_C(\tilde{x},0)[(1-y)+A_y y] \quad \tilde{x}=\text{constant}, \tag{5}$$

where $\tilde{x}$ and $\tilde{y}$ are fixed values of x and y, respectively. the coefficient A_x is given by $A_x=T_C(1,0)/T_C(0,0) =\beta_T N_T\mu_T^2/\beta_Z N_Z\mu_Z^2$, where the subscripts T and Z correspond to pure $PbTiO_3$ and $PbZrO_3$, respectively. In such a way we are sure to obtain the T_C of the pure compounds in the extremes of the phase diagram ($x=0,1$). No such simple relation can be written for A_y due to the reasons commented upon below. However, A_y can be understood as a fitting parameter analogous to A_x. In Fig. 3(a), the experimental values of $T_C(x,\tilde{y})$ vs x are represented by different symbols, along with the linear least-squared fits, plotted as full lines. It may be noted that the slopes are very similar for $y=0.026$

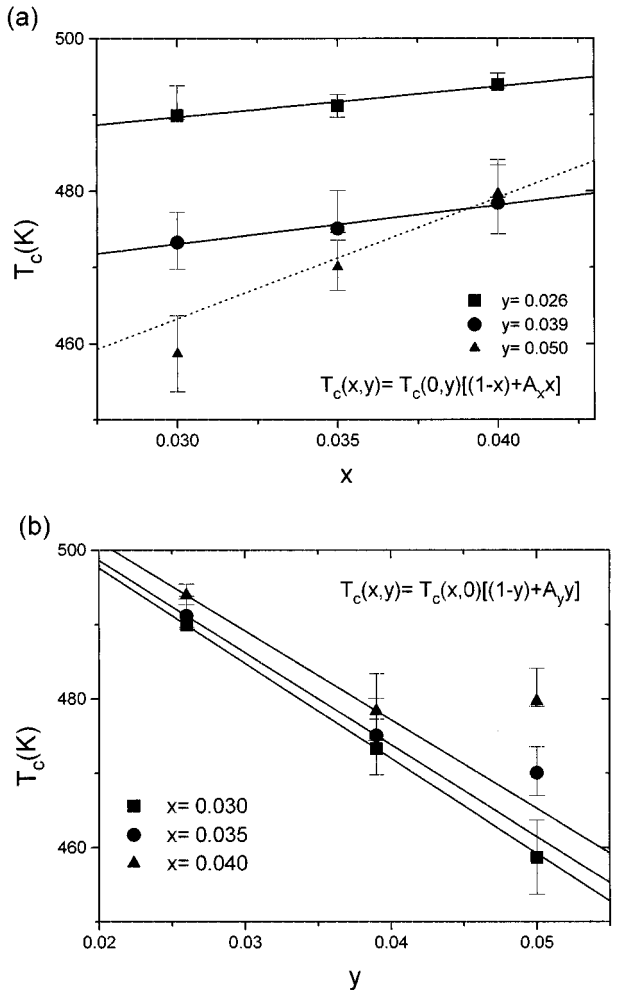

FIG. 3. Plot of the Curie temperature T_C vs X (a) and y (b). The full lines are best fits to Eqs. (4) and (5) which are combined into Eq. (6). Points with different symbols are experimental data.

and $y=0.039$, which indicates that the coefficient A_x is almost composition independent for $y<0.04$. Table II gives numerical values for A_x extracted from the experimental data fits.

For A_y we cannot confidently use Eq. (5) in the whole composition range (i.e., $0\leqslant y\leqslant 1$) because it is known that $PbNb_2O_6$ has the tungsten–bronze structure, which is quite different from the perovskite structure. Above the transition temperature, its paraelectric phase is not cubic but tetragonal. This means that Eq. (5) has no meaning in the high Nb range. However, we may expect that small Nb constants (<4 mol %, in our case) do not substantially change the perovskite structure, and, consequently, that we can use Eq. (5) to describe the dependence of $T_C(\tilde{x},y)$ vs y in the low Nb constant range. The numerical values for A_y obtained by fitting the experimental data are also given in Table II, where we find this coefficient is not too composition dependent for $y<0.04$. the experimental data for $T_C(\tilde{x},y)$ vs y and their linear least-squares fits are plotted in Fig. 3(b) by means of different symbols and full lines, respectively.

If we take into consideration the effects of x and y, simultaneously, on T_C the general expression for $T_C(x,y)$ is given, combining Eqs. (4) and (5), by

TABLE II. The calculated values for A_x and A_y in $T_C(x,y)=T_C(0,0)\times[(1-x)+A_x x][(1-y)+A_y y]$.

x(mol %)	A_x	y(mol %)	A_y
3.0	1.84	2.6	−3.27
3.5	2.12	3.9	−3.36
4.0	4.78	5.0	−3.44

$$T_C(x,y)=T_C(0,0)[(1-x)+A_x x][(1-y)+A_y y]. \quad (6)$$

We may conclude that Eq. (6) describes fairly well the x and y dependence of the Curie temperature for Nb-doped Zr-rich PZT.

On the other hand, we have defined, just before Eq. (2), the dimensionless parameter $g(x,y)$, which determines the more or less pronounced first-order character of the transition,[26] and is dependent on N^2, the squared number of dipoles per unit volume. Then, in an analogous way to that for $T_C(x,y)$, we get

$$g(x,\tilde{y})=g(0,\tilde{y})[(1-x)^2+B_x x^2], \quad \tilde{y}=\text{constant}, \quad (7)$$

$$g(\tilde{x},y)=g(\tilde{x},0)[(1-y)^2+B_y y^2], \quad \tilde{x}=\text{constant}, \quad (8)$$

and

$$g(x,y)=g(0,0)[(1-x)^2+B_x x^2][(1-y)^2+B_y y^2]. \quad (9)$$

Note that x and y are small in all of our cases, so the higher order terms involving xy, x^2y, xy^2, and x^2y^2 in the expansion of Eq. (9) are considerably smaller than the terms in x and y, unless the coefficients B_x and B_y are unexpectedly large. Neglecting terms of order higher than second order in x and/or y we get

$$g(x,y)\cong g(0,0)[1-2(x+y)+4xy+(B_x+1)x^2 + (B_y+1)y^2\cdots], \quad (10)$$

which indicates that, as a first approximation, $g(x,y)$, unlike $T_C(x,y)$, should show a linear dependence on $(x+y)$ in the range of our investigation.

Similarly, for parameter h, we have

$$h(x,y)=h(0,0)[(1-x)^4+C_x x^4][(1-y)^4+C_y y^4] \quad (11)$$

and

$$h(x,y)\cong h(0,0)[1-4(x+y)+16xy+6(x^2+y^2)\cdots], \quad (12)$$

which indicates that, as a first approximation, $h(x,y)$ should show a linear dependence on $(x+y)$ for $x,y\ll 1$.

We have used a set of data[21] in a more extended range of $(0.03\leqslant x\leqslant 0.09)$ at fixed $y=0.056$ to get $g(0,0)=0.59$, $h(0,0)=-0.12$, $B_x=1.04$, and $B_y=-1.70$ for a reasonable fit to our present set of data. The resulting values have estimated errors of at least 20%. The values for $g(0,0)$ and $h(0,0)$ are fully consistent with those obtained from hysteresis loops data.[27] We should make it clear that the different procedures used in previous works[21,27,28] to determine the dimensionless coefficients g and h, give consistently relatively well-defined values for g but lead to considerable uncertainties for h, and do not rule out the possibility that higher order coefficients are needed. These higher order

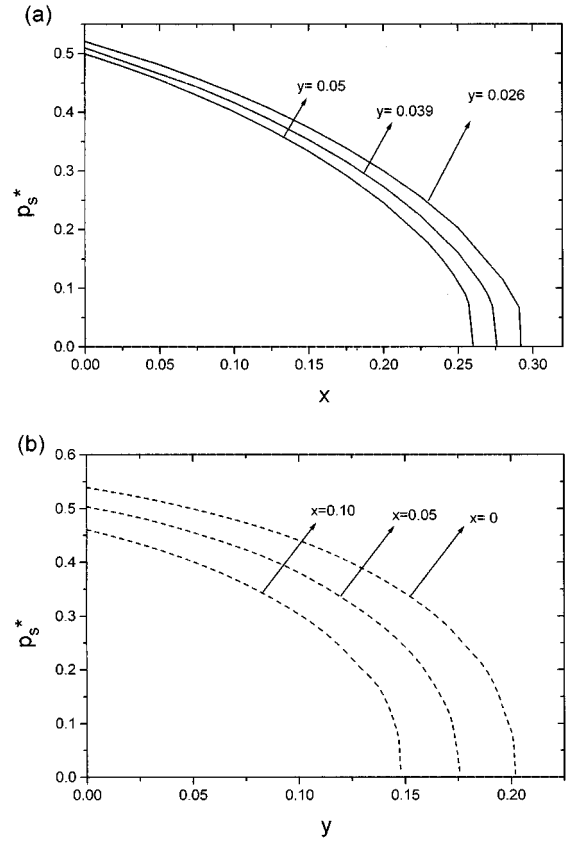

FIG. 4. Calculated composition dependence of the normalized spontaneous polarization, $p_s^* = P_s^*/P_{s0}$, at the $F_{RH}-P_C$ phase transition temperature: (a) p_s^* vs x for several values; (b) p_s^* vs y for several x values. Dashed lines are indicative because the y value is beyond our expected range of approximation.

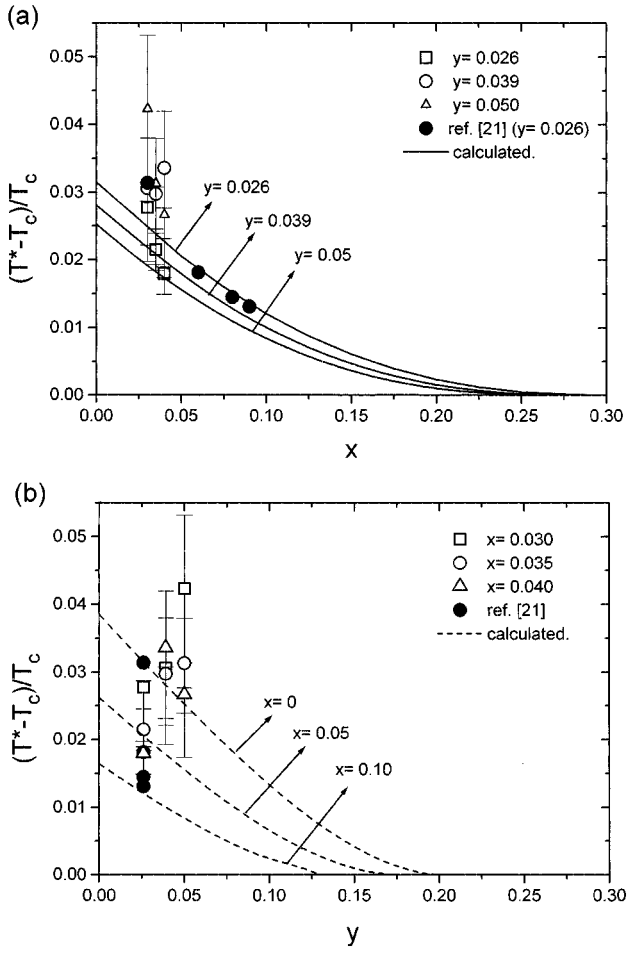

FIG. 5. Plot of $\Delta T/T_C$ vs (x,y) from Eqs. (3), (10), and (12) for different compositions (lines) together with the experimental data and those from Ref. 21: (a) $\Delta T/T_C$ vs x for different y values; (b) $\Delta T/T_C$ vs y for different x values. Dashed lines are indicative because the y value is beyond our expected range of approximation.

coefficients might result in higher $\Delta T/T_C$ at low x values, where our theoretical curves depart most from the data.

Substituting Eqs. (10) and (12) into Eq. (3) at the F_{RH} to P_C transition temperature (T^*) we get the relationship between (x,y) and p_s^*, plotted in Figs. 4(a) and 4(b). Also we can get numerically the calculated (x,y) dependence of $\Delta T/T_C$, which is plotted in Figs. 5(a) and 5(b). Full lines correspond to $g(0,0)=0.59$ and $h(0,0)=-0.12$, $B_x=1.04$, and $B_y=-1.70$ for $y=0.026$, 0.039, 0.050 and $x=0$, 0.05, 0.10, respectively. Also plotted are our experimental data and additional experimental data from Ref. 21.

B. Comments on the $F_{RL}-F_{RH}$ phase transition

As we have mentioned before a small amount of Nb content can change significantly the $F_{RL}-F_{RH}$ transition behavior and other characteristic properties such as the dielectric constant, the spontaneous polarization jump (ΔP_s), and the phase transition order. It is known that the spontaneous polarization discontinuity at the $F_{RL}-F_{RH}$ phase transition for 95/5 type PZT ferroelectric ceramics arises due to the cation (Pb and Zr/Ti/Nb ions) shifts along the ⟨111⟩ direction, because of the coupling effect between oxygen's octahedra tilt (η_s) and the spontaneous polarization (P_s). The spontaneous polarization discontinuity can be affected by the Ti and Nb content. What we are interested in is how the composition, x and y, affects the ΔP_s and the transition temperature.

Based on the generalized effective field approach, the spontaneous polarization change can be shown to be a function of p_s (normalized spontaneous polarization) and η_s (normalized spontaneous tilt angle) as follows.[27]

$$\Delta p_s = (1+p_s\eta_s)^{-1}(1-p_s^2)\,\eta_s\,. \tag{13}$$

In this equation, p_s and η_s are related to temperature through[28]

$$\frac{T}{T_C} = \frac{1+gp_s^2+hp_s^4}{\tanh^{-1}\,p_s/p_s} \tag{14}$$

and

$$\frac{T}{T_{CT}} = \frac{1+g_t\eta_s^2+h_t\eta_s^4}{\tanh^{-1}\,\eta_s/\eta_s}, \tag{15}$$

respectively.

In principle, T_C, T_{CT}, g, h, g_t, and h_t could be given in terms of the composition, x and y, in a similar way to that discussed above for the $F_{RH}-P_C$ transition. So, Eq.

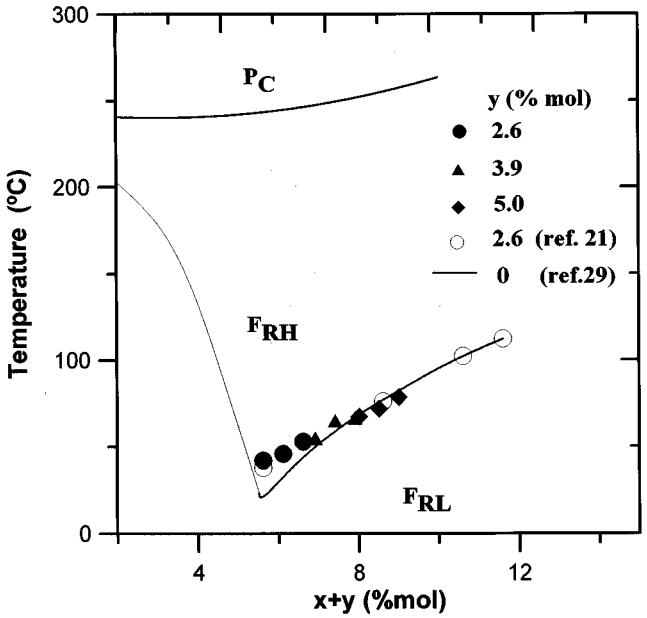

FIG. 6. The effects of Nb contents on the $F_{RL}-F_{RH}$ phase transition temperature T_{LH}. Different symbols correspond to different Nb contents and coincide with Jaffe's data without Nb content (full lines). This means that the $F_{RL}-F_{RH}$ transition temperature for small Nb content (in our case $\leqslant$5mol %), is well defined by the curve corresponding to pure PZT.

(13) could, in theory, describe the composition dependence of the spontaneous polarization discontinuity. We lack, however, enough experimental information to get it numerically. Sufficiently detailed measurements of ΔP_s for different compositions have not yet been performed. This is left for further study. At present we have only dielectric constant data, shown in Fig. 2 for different compositions. From them we can see that increasing Ti or Nb content increases, as is well known, the temperature at which the anomaly of the dielectric constant corresponding to the $F_{RL}-F_{RH}$ transition appears. An increase in the diffuse character with the increase of Nb content can also be seen. In Fig. 6 the $F_{RL}-F_{RH}$ transition temperatures are plotted versus $(x+y)$ with x being the Ti content and y the Nb content, for the compositions investigated in this work. The experimental data from Ref. 21, which correspond to $y=0.026$, and the phase boundary line for pure PZT[29] ($y=0$) have also been included. It can be seen that the $F_{RL}-F_{RH}$ phase boundary is almost unaffected by the substitution of Nb (y) instead of Ti (x), for small amounts of y ($<$5 mol %). This dependence supports the idea[20] that the Nb^{5+} ions substitute Zr^{4+} ions and that they are not located at interstitial positions.[19] This is also consistent with the observed[27] weak coupling between O_3 tilt (responsible for the $F_{RL}-F_{RH}$ transition) and the polarization.

IV. SUMMARY

In summary, in the range of small amount of Ti(x) and Nb(y) content, the Curie temperature of the Nb-doped PZT system can be described fairly well within the framework of an effective field approach for a combination of Ti and Nb content in the range $x \ll 1$, $y \ll 1$. The thermal hysteresis at the $F_{RH}-P_C$ transition can be described by means of higher order coefficients ($g,h,\ldots$), determinant of the phase transition character. The experimental errors in the determination of ΔT are considerable due to the diffuse character of the transition.

The behavior of the dielectric constant as a function of Ti(x) and Nb(y) at the $F_{RL}-F_{RH}$ transition has been characterized experimentally in the narrow range $0.03 \leqslant x \leqslant 0.04$, $0.026 \leqslant y \leqslant 0.05$, and the data indicate that the anomaly at T_{LH} becomes smoother and shifts toward higher temperature as the Nb content increases. The amount of shift in the phase boundary due to Nb doping (y) is equivalent to that due to Ti(x) substitution, a fact which is related to the secondary role of cation displacements in this transition. Our results provides useful information for choosing compositions for specific applications.

ACKNOWLEDGMENTS

We wish to acknowledge financial support from CICyT (Grant No. PB93-1253/94), Iberdrola (Grant No. INDES 94/95), Comunidad de Madrid (Grant No. AE00138-94, and CEAO (UAM).

[1] K. Roleder and J. Handerek, Phase Transit. **2**, 285 (1982).
[2] Y. L. Wang, Z. M. Cheng, Y-R Sun, and X-H. Dai, Physica B **150**, 168 (1988).
[3] M. J. Haun, E. Furman, S. J. Jang, and L. E. Cross, Ferroelectrics **99**, 13, 27, 45, 55, 63 (1989).
[4] V. A . Isupov, Ferroelectrics **143**, 109 (1993).
[5] H. M. Barnett, J. Appl. Phys. **33**, 1606 (1962).
[6] A. M. Glazer and S. A. Mabud, Acta Crystallogr. Sec. B **34**, 1060 (1978).
[7] X. H. Dai, J. F. Li, and D. Vieland, J. Appl. Phys. **77**, 3354 (1995).
[8] D. Viehland, J. F. Li, X. H. Dai, and Z. Xu, J. Phys. Chem. Solids **57**, 1545 (1996).
[9] B. Noheda, T. Iglesias, N. Cereceda, J. A. Gonzalo, H. T. Chen, Y. L. Wang, D. E. Cox, and G. Shirane, Ferroelectrics **184**, 251 (1996).
[10] X. Dai and Y-L. Wang, Phys. Status Solidi A **124**, 435 (1991).
[11] J. A. Gonzalo, Y. L. Wang, B. Noheda, G. Lifante, and M. Koralewski, Ferroelectrics **153**, 347 (1994).
[12] D. Xunhu and Y. L. Wang, Ferroelectrics **109**, 253 (1990).
[13] R. C. Buchanan, J. Huang, and J. E. Sundeen, Electroceramics V, Aveiro, Portugal, 2–4 September 1996 (unpublished), pp. 309.
[14] R. Gerson and H. Jaffe, J. Phys. Chem. Solids **24**, 979 (1963)
[15] S. Takahashi, Ferroelectrics **41**, 143 (1982).
[16] M. Hafid, G. E. Kugel, J. Handerek, and Z. Ujma, Ferroelectrics **135**, 101 (1992).
[17] W. L. Warren, J. Robertson, D. B. Dimos, B. A. Tuttle, and D. M. Smyth, Ferroelectrics **153**, 303 (1994).
[18] Y. L. Wang, New Ceram. **11**, 87 (1990) (in Japanese).
[19] L. Benguigui, J. Solid State Chem. **3**, 381 (1971).
[20] Z. Ujma, D. Dmytrów, and M. Pawelczyk, Ferroelectrics **120**, 211 (1991).
[21] B. Noheda, N. Cereceda, T. Iglesias, G. Lifante, J. A. Gonzalo, H. T. Chen, Y. L. Wang, D. E. Cox, and G. Shirane, Phys. Rev. B **51**, 16 388 (1995).
[22] M. Yokosuka and M. Marutake, Jpn. J. Appl. Phys. 1 **25**, 981 (1986).
[23] V. A. Isupov, Ferroelectrics **143**, 109 (1993).
[24] A. A. Bokov, Solid State Commun. **90**, 687 (1994).
[25] J. A. Gonzalo, *Effective Field Approach to Phase Transitions and Some Applications to Ferroelectrics* (World Scientific, Singapore, 1991).
[26] N. Cereceda, N. Duan, B. Noheda, and J. A. Gonzalo, in Ref. 13, p. 193.
[27] N. Cereceda, B. Noheda, T. Iglesias, J. R. Fernández-del-Castillo, J. A. Gonzalo, N. Duan, and Y. L. Wang, Phys. Rev. B **55**, 6174 (1997).
[28] N. Duan, N. Cereceda, B. Noheda, and J. A. Gonzalo, Ferroelectr. Lett. Sect. **22**, 27 (1996).
[29] B. Jaffe, W. R. Cook, Jr., and H. Jaffe, *Piezoelectric Ceramics* (Academic, London, 1971).